Engelborghs, Y. (1981) *J. Biol. Chem. 256*, 3276-3278.
Engelborghs, Y., & Fitzgerald, T. J. (1987) *J. Biol. Chem. 262*, 5204-5209.
Gallela, G., & Smith, D. (1982) *Can. J. Biochem. 60*, 71-80.
Garland, D. L. (1978) *Biochemistry 17*, 4266-4272.
Hamel, E., & Lin, C. M. (1984) *Biochemistry 28*, 2662-2667.
Hastie, S. B., Williams, R. C., Jr., Puett, D., & MacDonald, T. L. (1989) *J. Biol. Chem. 264*, 6682-6688.
Kasha, M. (1949) *J. Opt. Soc. Am. 38*, 929-934.
Lambeir, A., & Engelborghs, Y. (1981) *J. Biol. Chem. 256*, 3279-3282.
Luduena, R. F., Shooter, E. M., & Wilson, L. (1977) *J. Biol. Chem. 252*, 7006-7014.
Maity, S. N., & Bhattacharyya, B. (1987) *FEBS Lett. 218*, 102-106.
Mejillano, M. R., & Himes, R. H. (1991) *J. Biol. Chem. 266*, 657-664.
Sackett, D. L., Zimmerman, D. A., & Wolff, J. (1989) *Biochemistry 28*, 2662-2667.
Sioussat, T. M., & Boekelheide, K. (1989) *Biochemistry 28*, 4435-4443.
Watanabe, T., & Flavin, M. (1973) *Fed. Proc. 32*, 642.
Wilson, L., & Friedkin, M. (1966) *Biochemistry 5*, 2463-2468.
Wolff, J., Knipling, L., Cahnmann, H. J. & Palumbo, G. (1991) *Proc. Natl. Acad. Sci. U.S.A. 88*, 2820-2824.
Zaremba, T. G., LeBon, T. R., Millar, D. B., Funejkal, R. M., & Hawley, R. J. (1984) *Biochemistry 23*, 1073-1080.
Zweig, M. H., & Chignell, C. F. (1973) *Biochem. Pharmacol. 23*, 2142-T973.

Errors in RNA NOESY Distance Measurements in Chimeric and Hybrid Duplexes: Differences in RNA and DNA Proton Relaxation†

Andy C. Wang,‡ Seong G. Kim,§,∥ Peter F. Flynn,§,⊥ Shan-Ho Chou,# John Orban,§,▽ and Brian R. Reid*,‡,§

Biochemistry Department, Chemistry Department, and Howard Hughes Medical Institute, University of Washington, Seattle, Washington 98195

Received November 15, 1991; Revised Manuscript Received February 10, 1992

ABSTRACT: Nuclear magnetic resonance experiments reveal that the base H8/H6 protons of oligoribonucleotides (RNA) have T_1 relaxation times that are distinctly longer than those of oligodeoxyribonucleotides (DNA). Similarly, the T_1 values for the RNA H1′ protons are approximately twice those of the corresponding DNA H1′ protons. These relaxation differences persist in single duplexes containing covalently linked RNA and DNA segments and cause serious overestimation of distances involving RNA protons in typical NOESY spectra collected with a duty cycle of 2-3 s. NMR and circular dichroism experiments indicate that the segments of RNA maintain their A-form geometry even in the interior of DNA-RNA-DNA chimeric duplexes, suggesting that the relaxation times are correlated with the type of helix topology. The difference in local proton density is the major cause of the longer nonselective T_1s of RNA compared to DNA, although small differences in internal motion cannot be completely ruled out. Fortunately, any internal motion differences that might exist are shown to be too small to affect cross-relaxation rates, and therefore reliable distance data can be obtained from time-dependent NOESY data sets provided an adequately long relaxation delay is used. In hybrid or chimeric RNA-DNA duplexes, if the longer RNA relaxation times are not taken into account in the recycle delay of NOESY pulse sequences, serious errors in measuring RNA proton distances are introduced.

Modern molecular biology research has greatly expanded our knowledge of RNA function in recent years (Hoffman, 1991). Like proteins, RNA performs a wide variety of structural and functional roles, ranging from transfer RNA molecules, with their distinctive cloverleaf structures, to the replicating "killer toxin"-encoding double-stranded yeast RNA (Wickner et al., 1986). In addition, RNA carries the genetic transcript as messenger RNA, is found in association with proteins [e.g., ribosomes, spliceosomes, and RNaseP (Guerrier-Takada et al., 1983)], and has been found to self-splice and act as a catalyst (Cech & Bass, 1986). It also plays a role in gene regulation as antisense RNA (Green et al., 1986) and is the genetic material of many families of viruses (e.g., retroviruses). Recent advances in solid-state phosphoramidite chemistry have made it possible to routinely synthesize very pure RNA oligomers (Ogilvie et al., 1988) in NMR quantities (Chou et al., 1989). Thus defined sequence DNA-RNA hybrids are now amenable to structural investigation using NMR techniques. Indeed, because the strategies for DNA and RNA synthesis are compatible, one can study not only

† This investigation was supported by Grants GM32681 and GM42896, awarded by the National Institute of Health, U.S. Public Health Service.

* Address correspondence to this author.
‡ Biochemistry Department, University of Washington.
§ Chemistry Department, University of Washington.
∥ Present address: Center for Magnetic Resonance, University of Minnesota, Minneapolis, MN 55455.
⊥ Present address: Hare Research Incorporated, 18943 120th Ave. N.E., Suite 104, Bothell, WA 98011.
Howard Hughes Medical Institute, University of Washington.
▽ Present address: Center for Advanced Research in Biotechnology, Rockville, MD 20850.

0006-2960/92/0431-3940$03.00/0

hybrids, which are important in gene transcription, but also covalently linked DNA–RNA chimeras which occur in DNA replication (e.g., Okazaki fragments). RNA segments inserted into DNA duplexes appear to maintain their A-form structure (Chou et al., 1991), making such covalent chimeras useful models for A/B junctions in DNA. The possibility of a B-DNA/A-DNA junction in vivo was suggested by Rhodes and Klug (1986), who, on the basis of the observation that the *Xenopus* transcriptional factor IIIa (TFIIIA) can bind to both the 5S RNA transcript of the gene and to the DNA of the structural gene itself, proposed that the DNA site for TFIIIA in the *Xenopus* genome has an A-like structure. From Raman spectroscopic studies of synthetic DNA oligomers in the solid state and in solution (Peticolas et al., 1988; Wang et al., 1987), it was found that this sequence contains determinants for forming an A-form structure in solution. In light of the important role which A-form/B-form junctions might play in gene regulation, we have begun studies on the structure of A/B junctions using RNA–DNA chimeras. NMR studies on such covalent RNA–DNA duplexes are likely to increase rapidly in the future.

In determining the quantitative three-dimensional solution structure of nucleic acid duplexes, the general approach is to derive a set of proton–proton distance estimates from the initial-rate NOE buildup of assigned NOESY cross-peaks using reference cross-peaks separated by a known fixed distance (e.g., the cytosine H5–H6 cross-peak). These distances may then be used in distance geometry or molecular dynamics algorithms to generate coordinates that are consistent with the experimentally derived distances. The coordinates are then refined to correct for spin-diffusion errors (indirect magnetization transfer) by back-calculation spectral simulation methods, or relaxation matrix methods, until the simulations match the experimental NOESY spectra. Both the structure-generating (distance measurement) and trial structure NOESY simulation phases of the above approaches involve certain assumptions. Among the more important of these is the assumption of similar motional behavior for the protons, i.e., that all proton pairs in the molecule have essentially the same internal correlation time as the fixed reference proton pair. The second (isotropic) assumption is that the internuclear vector orientation (polar angle) does not affect the NOE cross-relaxation rate; while longer duplexes (length:diameter > 2:1) obviously undergo rotational diffusion about the helix axis more rapidly than end-over-end diffusion, the isotropic approximation appears valid for 10–12 bp duplexes, and in such duplexes the maximum distance error due to differences in internuclear vector orientation is always less than 10%, even in the worst case where the reference proton pair has a polar angle of 90° and the other proton pair has a polar angle of 0° (Wang et al., 1992). The third important assumption in calculating distances, or in matching experimental and simulated intensities, is that the entire spectrum is fully relaxed—or at least that all proton pairs are *equally* relaxed, i.e., they all have the same fractional polarization as the fixed reference proton pair. In practice, the relaxation delay is the longest component of the signal-averaging duty cycle and is generally minimized to avoid prohibitively long NOESY experiments. Hence, the longitudinal T_1 relaxation rates for all protons, including reference protons, are generally assumed to be the same, or very similar; if they are not, then appreciably longer T_1s (incomplete recovery) will lead to overestimated distances (weaker NOEs) for those particular protons. Thus, in addition to the effects of internal motion (amplitude, time scale) on cross-relaxation, the effects of different longitudinal T_1 relaxation among the various protons can also lead to weaker apparent NOEs and errors in distance estimates.

In the present study, anomalously weak NOEs were observed from the RNA protons of chimeric duplexes (which lead to errors in overestimating the corresponding distances). These errors were found to be due to differential proton packing densities rather than motion or anisotropy and can be eliminated by extended relaxation delays in the NOESY pulse sequences.

Materials and Methods

(*a*) *Sample Preparation.* The DNA dodecamers [d(CGCGAAUUCGCG)]$_2$ and [d(CGCGUAUACGCG)]$_2$ were synthesized on a 10-μmol scale by using solid-phase phosphoramidite techniques as described previously (Hare et al., 1983). The RNA dodecamers [r(CGCGAAUUCGCG)]$_2$ and [r(CGCGUAUACGCG)]$_2$ were synthesized as previously described (Ogilvie et al., 1988; Chou et al., 1989). The synthesis of the chimeras [d(CGCG)r(AAUU)d(CGCG)]$_2$ and [d(CGCG)r(UAUA)d(CGCG)]$_2$ has been described elsewhere (Chou et al., 1991). The 5A and 6A 2″-deuterium-labeled sample [d(CGCGA*A*TTCGCG)]$_2$ was synthesized as described previously (Huang et al., 1990). The crude DNA was purified as described by Kintanar et al. (1987) and lyophilized to dryness. Each purified lyophilized duplex was dissolved in 0.4 mL of buffer containing 200 mM sodium chloride and 20 mM sodium phosphate at pH 7.0 and repeatedly lyophilized to dryness, first from the aqueous buffer and then from D_2O solution. Finally, 0.4 mL of 99.996% D_2O was added, and the solution was transferred to a 5-mm NMR tube. For the NOESY experiments, about 20 mg of sample was used, i.e., the concentration was 45 mg/mL or approximately 6.5 mM in duplex. The longitudinal and transverse relaxation experiments were carried out at a concentration of ca. 7.5 mg/mL or approximately 1 mM in duplex. The circular dichroism experiments were carried out at a further 10-fold dilution, i.e., 0.1 mM in duplex.

(*b*) *Cross-Relaxation Experiments.* The time-dependent NOESY experiments in D_2O were acquired on a home-built NMR spectrometer operating at 500 MHz for protons (Gladden and Drobny, unpublished results). The sample temperature was regulated at 29 °C for all experiments. Five NOESY spectra with mixing times of 0.03, 0.06, 0.09, 0.12, and 0.18 s were all collected within a single 5-day period without removing the sample from the spectrometer or changing any frequencies or gain settings. The pure absorption NOESY spectra were collected using phase-sensitive methods (States et al., 1982) into 1024 complex points in t_2 with 400 points in t_1. For each t_1 experiment, 32 scans were collected with a relaxation delay of 2.0 s between transients. Three additional NOESY spectra were also collected with mixing times of 0.03, 0.06, and 0.18 s, with a relaxation delay of 10.0 s.

(*c*) *Longitudinal Relaxation Experiments.* Nonselective inversion–recovery experiments were acquired on a Bruker AM-500 spectrometer. The temperature was regulated at 29 °C for all experiments with spinning at 20 Hz; the HDO peak was not presaturated. A composite $90°_x$–$180°_y$–$90°_x$ inversion pulse was used since this accurately inverts spins over a wider range of chemical shifts than a simple 180° pulse (Ernst et al., 1987). The free-induction decay (FID) was collected into 4096 complex points. Twenty-five variable delays (τ) were used between the inversion pulse and the observe pulse; six of the variable delays were less than 0.1 s. For each time point, 64 scans were collected with a relaxation delay of 15.0 s. The data were fitted with a three-parameter expression (Bruker

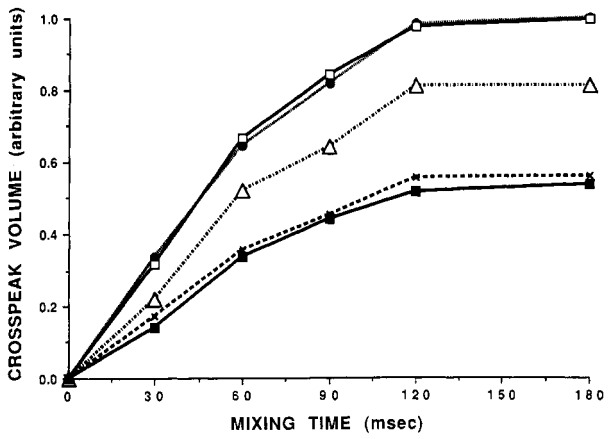

FIGURE 1: H5-H6 NOESY cross-peak buildups. H5–H6 cross-peak intensity volume integrals are plotted as a function of mixing time using a 2-s recycle delay: dC3, solid circles; dC11, open squares; dC9, open triangles; rU7, solid squares; rU8, crosses. The volume errors are ca. ±10%.

Aspect 3000 software): $S(t) = A + Be^{-t/T_1}$. For each sample, the T_1 experiment was performed at least twice; the standard deviation was ca. 0.08.

(*d*) *Transverse Relaxation Experiments.* All transverse relaxation experiments were performed on a Bruker AM-500 spectrometer; the temperature was 29 °C for all experiments. The HDO peak was not presaturated, and a nonspinning sample was used to avoid echo modulation. The FID was collected into 4096 complex points. Various T_2 methods were tried, but the Levitt and Freeman (1981) pulse sequence $90°_x-[\tau-90°_x180°_y90°_x-\tau]c$ (where c is the number of times the composite pulse is executed) was found to be by far the most reliable method for determining T_2 (Table I). Only even-numbered echos were collected. A total of 41 time points were sampled in a random order, and, for each time point, 64 scans were collected with a relaxation delay of 15.0 s. The data were fitted with a single exponential (Bruker Aspect 3000 software): $S(t) = Ae^{-t/T_2}$. Each experiment was performed twice for all samples; the standard deviation was ca. 0.13.

(*e*) *Circular Dichroism Experiments.* The CD spectra were acquired on a JASCO 720 spectrometer at room temperature. The bandwidth was 1.0 nm, the sensitivity was 0.02°, and the response was 0.5 s. The scan speed was set at 100 nm/min with a step resolution of 0.2 nm. Ten scans were summated for each sample. The CD spectrum of the buffer was subtracted from the CD spectra of the samples to obtain the response due to the solute molecules alone. Finally, the spectra were subjected to a JASCO noise-reduction software process.

RESULTS

The NOESY initial-rate buildups for the H5–H6 cross-peaks of dC and rU residues in the chimera [d(CGCG)r(AAUU)d(CGCG)]$_2$ are shown in Figure 1; these data were acquired using a relaxation delay of 2 s. The apparent H5–H6 cross-relaxation rates (R_C) for rU7 and rU8 are approximately half those of dC3 and dC11 while the H5–H6 R_C of dC9 (a DNA/RNA junction residue) is intermediate. If the assumptions of similar motion and similar relaxation (equilibrium magnetization) described above are valid, this observation gives rise to the surprising (and impossible) conclusion that uracil H5–H6 distances in the RNA segment are ca. 2.83 Å compared to ca. 2.52 Å for the cytosine H5–H6 distances in DNA. Since the H5–H6 distances are actually very similar, i.e., 2.46 Å in uracil (McMullan & Craven, 1989) and 2.52 Å in cytosine (Weber et al., 1980), the marked differences in *initial* slopes (R_C) must be due to differences in either equilibrium magnetization or spectral density (internal motion). Before any structural studies can be undertaken on such a DNA–RNA–DNA chimera, it is essential to establish the source of the differences in apparent cross-relaxation between the DNA and the RNA residues. Longitudinal and transverse relaxation data were obtained for the pure DNA, pure RNA, and chimeric samples in an effort to determine the source of the R_C differences between pyrimidines in [d(CGCG)r(AAUU)d(CGCG)]$_2$. Figure 2A,B shows inversion–recovery stack plots of the anomeric H1′ protons in [d(CGCGAAUUCGCG)]$_2$ compared to [r(CGCGAAUUCGCG)]$_2$. The null point for the DNA anomeric protons occurs at approximately 1.5 s, at which time the RNA protons are still inverted, while the RNA anomeric protons have a null point at ca. 2.2 s. Furthermore, after 4 s of recovery, the RNA protons exhibit only ca. 50% of their equilibrium intensity whereas the corresponding DNA anomeric protons are essentially fully recovered. The fact that these spectra have been assigned (Chou et al., 1989, 1991) allowed us to monitor the anomeric proton relaxation at each position in the RNA and DNA duplexes. In Figure 3A the inversion–recovery T_1 values for the 12 anomeric H1′ protons are plotted for the RNA duplex [r(CGCGAAUUCGCG)]$_2$ and the corresponding DNA duplex [d(CGCGAAUUCGCG)]$_2$ containing dU instead of dT at positions 7 and 8. The analogous H1′ T_1 data for the duplexes [r(CGCGUAUACGCG)]$_2$ and [d(CGCGUAUACGCG)]$_2$ are plotted in Figure 3B. Two important points emerge: (a) anomeric proton T_1s vary within pure DNA by ca. 1.5-fold and within pure RNA by ca. 3.3-fold as a function of position in the sequence, and (b) it is immediately obvious that the H1′ values are 2–3 times longer in RNA, regardless of sequence.

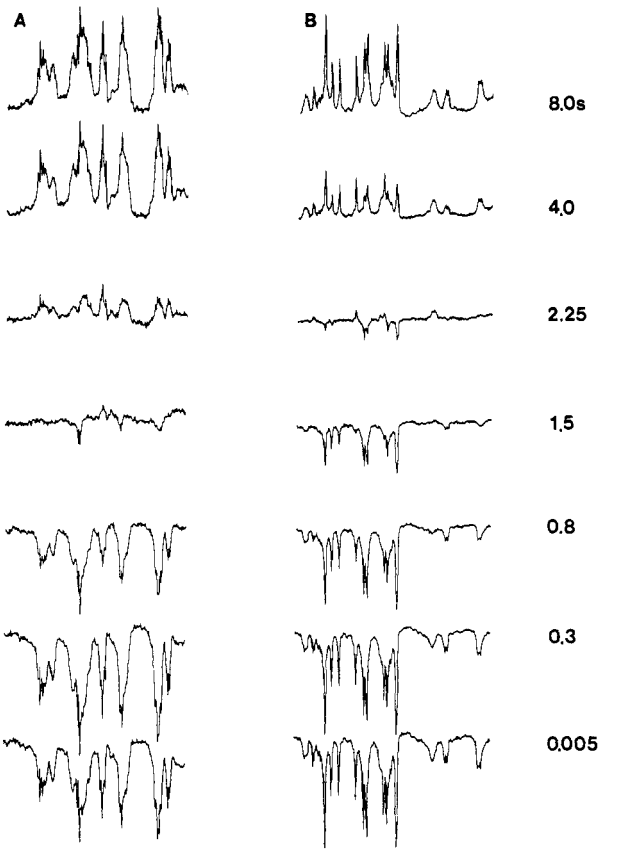

FIGURE 2: Inversion–recovery data on [(CGCGAAUUCGCG)]$_2$. Stack plots of inversion–recovery data for (A) [d(CGCGAAUUCGCG)]$_2$ and (B) [r(CGCGAAUUCGCG)]$_2$ in the anomeric H1′ region. The time delays between the inversion and the observation pulses are indicated alongside each trace.

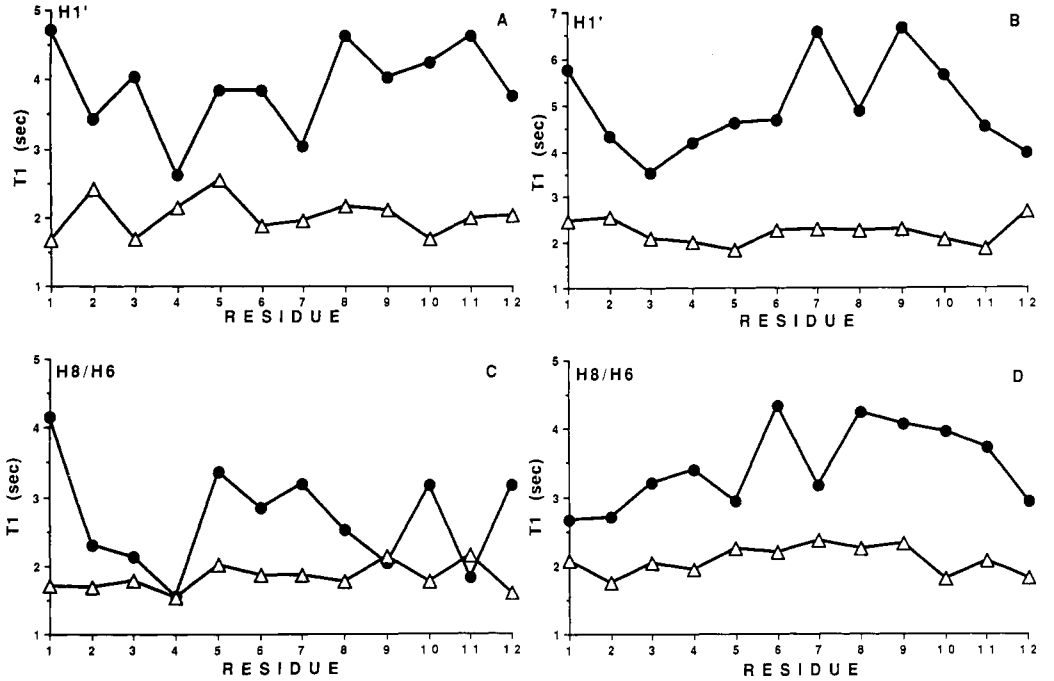

FIGURE 3: Residue-specific T_1 values in DNA and RNA duplexes. Nonselective T_1 values are given for (A) the anomeric sugar protons of $[CGCGAAUUCGCG]_2$, (B) the anomeric sugar protons of $[CGCGUAUACGCG]_2$, (C) the base H6 and H8 protons of $[CGCGAAUUCGCG]_2$, and (D) the base H6 and H8 protons of $[CGCGUAUACGCG]_2$. The solid circles are the RNA relaxation times, and the open triangles are the relaxation times of DNA protons. The data were collected and processed as described in the text. The standard deviation is ca. 8.0%.

Both observations could have either a structural or a motional explanation. The longer RNA T_1 relaxation also holds for the base H6/H8 protons (Figures 3C,D), although somewhat less dramatic than the H1′ relaxation differences. Indeed, RNA anomeric proton nonselective T_1s can be more than 3-fold longer than those of DNA in the cases of U7 and C9 in the sequence $[(CGCGUAUACGCG)]_2$. Residue G4 in $[(CGCGAAUUCGCG)]_2$ is a somewhat special case in that experiments have recently demonstrated metal ion binding at this position resulting in paramagnetic relaxation of the G4 H8 and H1′ protons (Jeff Davis, personal communication). Although sequence-specific metal ion binding data on RNA duplexes are lacking, the T_1 values in Figure 3A,C are consistent with rG4-specific paramagnetic relaxation. Interestingly, in chimeric d–r–d dodecamer duplexes containing four central RNA base pairs flanked by four DNA pairs on each side, the central ribonucleotides exhibit long RNA-like T_1s (3–6 s) while the flanking deoxyribonucleotides exhibit short (2–2.5 s) DNA-like T_1s for both the H1′ and H8/H6 protons (Figure 4).

Before structural studies on a chimera can begin, it is important to examine the possible mechanisms that might lead to T_1 differences between DNA and RNA. From eq 1 (Solomon, 1955)

$$\frac{1}{T_1} = \sum_{S \neq I} \frac{\hbar^2 \gamma_I^2 \gamma_S^2}{20 r_{IS}^6} [3J_1(\omega_I) + 12J_2(\omega_I + \omega_S)] \quad (1)$$

it is clear that one main contributor to nonselective T_1 relaxation is spin density (proton packing). RNA differs from DNA in at least two important structural properties that are likely to contribute, at least partially, to the slower relaxation behavior of RNA base and H1′ protons. First, one of the deoxyribose geminal protons in DNA (H2″) has been replaced by a hydroxyl group (OD in D_2O). The H2″ is the closest neighbor of the H1′, and one of the closest neighbors of the $(n + 1)$ H8/H6, in B-DNA. To test the influence of the H2″ proton on the T_1 of proximal protons in DNA, a nonselective inversion–recovery experiment was performed on a sample in

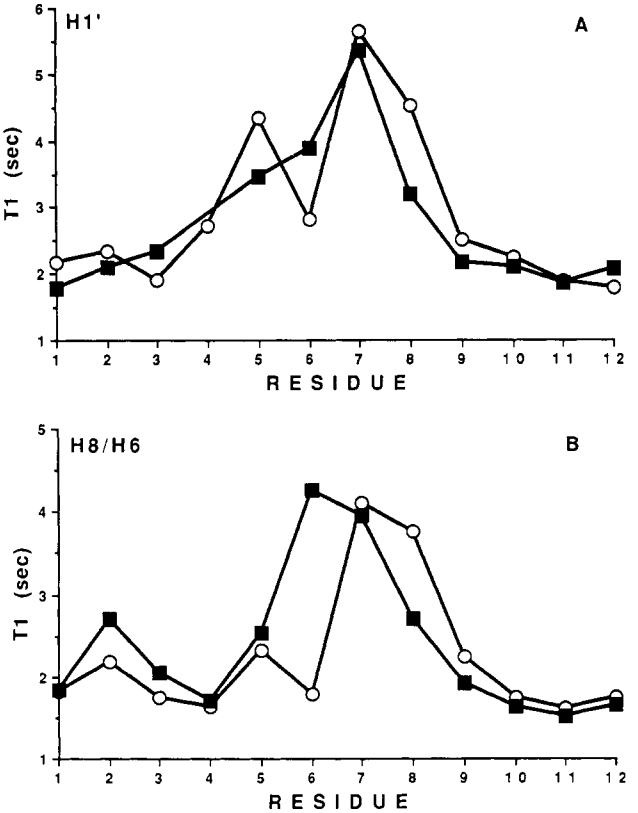

FIGURE 4: Longitudinal relaxation times in chimeric DNA–RNA–DNA duplexes. Nonselective T_1s are given for (A) the anomeric protons and (B) the base H6 and H8 protons. The open circles are the relaxation times for $[d(CGCG)r(AAUU)d(CGCG)]_2$, whereas the solid squares are the relaxation times for $[d(CGCG)r(UAUA)d(CGCG)]_2$. The data were collected and processed as described in the text. The standard deviation is ca. 8.0%.

which the 5A and 6A sugar 2″H protons were replaced by 2″D deuterons (Figure 5). Selective H2″ deuteration at 5A and 6A does increase the T_1 of the proximal A5H8, A6H8, T7H6, A6H1′, and T7H1′ protons to varying extents, but only par-

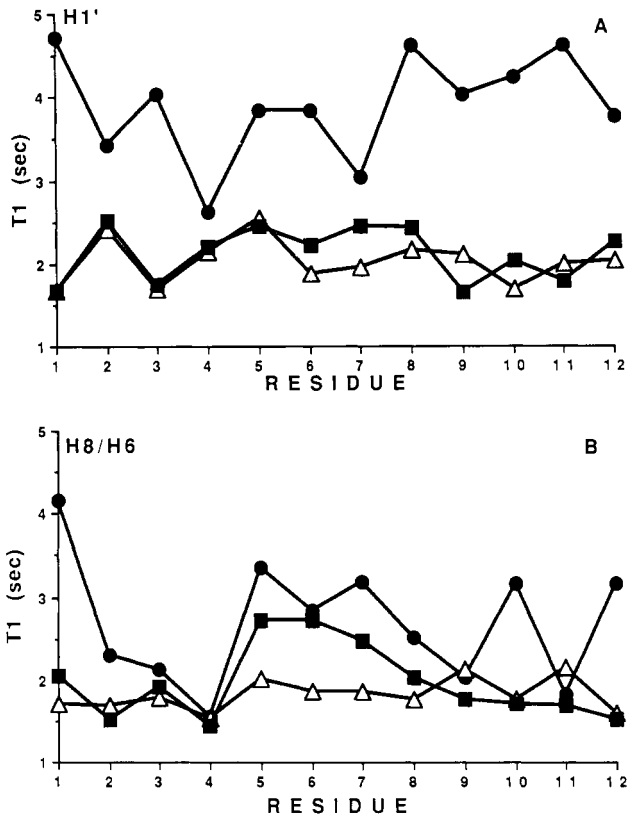

FIGURE 5: Longitudinal relaxation in $[r(CGCGAAUUCGCG)]_2$, $[d(CGCGAAUUCGCG)]_2$, and $[d(CGCGA^*A^*TTCGCG)]_2$. Nonselective T_1s of (A) the anomeric protons and (B) the base H6 and H8 protons are given. The RNA relaxation times, unlabeled DNA relaxation times, and deuterium-labeled DNA relaxation times are represented by solid circles, open triangles, and solid squares, respectively. In $[d(CGCGA^*A^*TTCGCG)]_2$, the H2" of dA5 and dA6 is replaced by deuterium. The standard deviation is ca. 8.0%.

Table I: T_2 Values from Various Experimental Methods (in ms)[a]

proton	line width	Hahn echo	CPMGLF
7U H1′	82	98	140
6A H1′	55	68	170
2G H8/8A H8	68	63	104
12G H8	64	63	104
10G H8	64	59	107
6A H8	71	60	103
6A H2	107	155	139
8A H2	111	166	166

[a] Line widths were measured at half-height and using the relationship $\Delta\nu_{1/2} = 1/(\pi T_2)$; the HSE experiment was performed using the pulse sequence RD–90°–τ–180°–τ–FID; and the CPMGLF experiment was performed as described in the text. The standard deviation for the CPMGLF T_2 was the lowest, with a standard deviation of ca. 13.5%. The sample used was $[d(CGCG)r(UAUA)d(CGCG)]_2$.

tially and not up to the long T_1 values of RNA. Second, the H5′,H5″ geminal proton pair is spatially removed by at least an extra 1.0 Å from nearest H1′ in A-form duplexes compared to B-form duplexes (i.e., from 3.2 → 4.6 Å) (Arnott & Hukins, 1972a,b), as a result of the different helical backbone geometries. Thus, one of the contributors to relaxing the DNA H1′ (i.e., the H2″) is not available for RNA H1′ protons, and another potential relaxation source (H5′ and H5″) is probably less efficient because of the increased distance between H1′ and the H5′,H5″ protons in RNA. As a separate illustration of how spin density alone can affect T_1 relaxation without invoking motion, one needs only to consider the T_1 values of the H2 and H8 protons on adenine residues in DNA. The rather isolated H2 proton has a T_1 value approximately 1.5 times as long as the H8 proton, even within a single adenine;

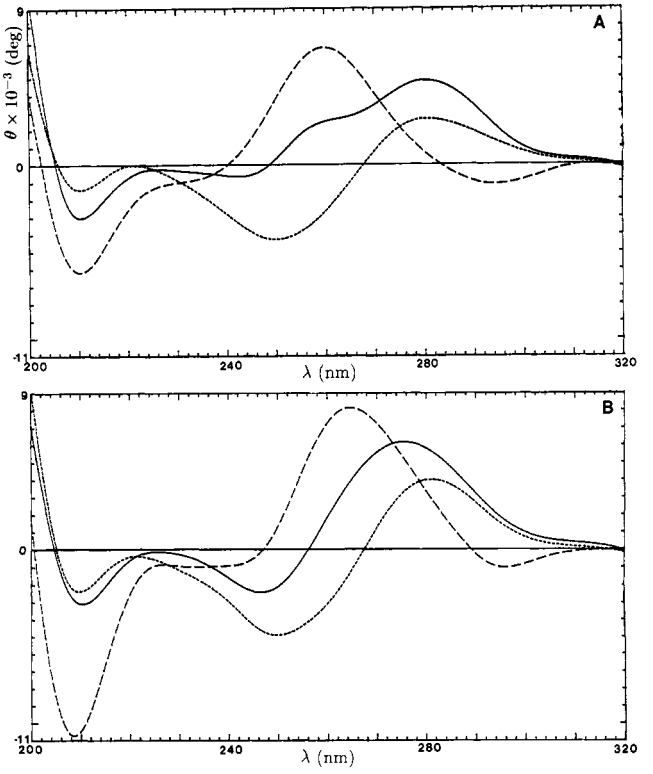

FIGURE 6: Circular dichroism spectra of (A) $[CGCGUAUACGCG]_2$ and (B) $[CGCGAAUUCGCG]_2$. The dashed curves are the RNA duplex spectra, the dotted lines are the DNA duplex CD spectra, and the solid lines are the spectra of the chimeras.

this cannot be due to differences in motion and must simply reflect the greater proton density around the H8. Spin density differences between adenine H2 and H8 protons also lead to T_2 differences, as shown in Table I.

These purely structural arguments can only fully explain the longer RNA T_1 in chimeric duplexes if the RNA segments maintain their A-like conformation; it became important, therefore, to determine whether the DNA and RNA moieties retain their individual secondary structures in mixed duplexes. To establish whether the RNA segments exhibit A-type geometry in d–r–d chimeras, we have carried out preliminary CD studies on d–d, r–r, and d–r–d duplexes. As shown in Figure 6 for the sequences $[(CGCGUAUACGCG)]_2$ and $[(CGCGAAUUCGCG)]_2$, the d–d dodecamer duplexes exhibit typical B-form CD spectra (Ivanov et al., 1973) while the r–r duplexes exhibit typical A-form CD spectra (Ivanov et al., 1973); however, the d–r–d chimera CD spectra exhibit both A-character and B-character, suggesting that the RNA segments do indeed maintain their A-type geometry. This conclusion is also supported by high-resolution NMR studies (Chou et al., 1991).

The second main contributors to nonselective T_1 relaxation are the single- and double-quantum spectral densities (eq 1). Spectral density is a function of both the internuclear vector orientation and molecular motion (global and/or internal). The time-dependent NOESY experiment can be used to detect any gross differences in motion/orientation between the RNA and DNA residues in the chimera. By observing the buildups of proton pairs separated by the same distance in DNA and RNA, differences in spectral density, and hence motion/orientation, can be monitored. We therefore collected three NOESY spectra at mixing times of 30, 60, and 180 ms using a much longer (10 s) relaxation delay to allow ≥75% recovery of even the slowest RNA proton. The 10-s RD NOESY H5-H6 cross-peak buildup rates for [d(CGCG)r(AAUU)d-

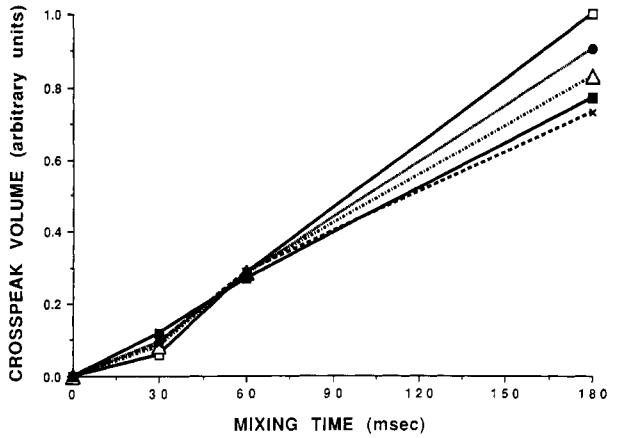

FIGURE 7: H5–H6 NOESY cross-peak buildups with long relaxation delay. H5–H6 cross-peak volumes are plotted as a function of mixing time using a 10-s recycle delay: dC3, solid circles; dC11, open squares; dC9, open triangles; rU7, solid squares; rU8, crosses. The volume errors are ca. ±10%.

$(CGCG)]_2$ are shown in Figure 7; in contrast to Figure 1, no significant differences in cross-relaxation rates were observed between any of the DNA or RNA pyrimidine H5–H6 proton pairs. Thus, the reduced H5–H6 cross-peak intensities for rU7 and rU8 in $[d(CGCG)r(AAUU)d(CGCG)]_2$ spectra collected with a 2-s relaxation delay (see Figure 1) are mainly caused by differential partial saturation effects, not differences in internal motion/orientation. When the RD is only 2 s, the DNA protons are ~63% recovered while RNA protons are only ~33% recovered and generate weaker NOE cross-peaks for the same standard distance; after a 10-s RD all protons are ≥75% recovered. If there were significant internal motion/orientation differences between the DNA and RNA H5–H6 internuclear vectors, their NOESY cross-peak buildups would be different, even after long relaxation delays. However, at 30 and 60 ms, they are indistinguishable, as shown in Figure 7. Thus, any internal motion differences that might exist between DNA and RNA are too small affect cross-relaxation rates, and therefore reliable distance measurements can be obtained from time-dependent NOESY data on hybrid/chimeric DNA–RNA samples *provided* that an adequately long relaxation delay is used.

Discussion

Compared to the number of NMR studies on DNA solution structure and dynamics, analogous studies on RNA are relatively scarce, due largely to earlier difficulties in synthesizing such molecules. The absence of information on whether RNA relaxation behavior is similar to, or different from, that of DNA could potentially compromise the determination of solution structures for RNA, DNA–RNA hybrids, and DNA–RNA–DNA chimeras. Because the elucidation of solution structures for hybrids and chimeras by NMR is in its infancy, we undertook a comparative study of the relaxation properties of DNA, RNA, and chimeric duplexes in solution. The samples used in this study include the chimeric duplexes $[d(CGCG)r(AAUU)d(CGCG)]_2$ and $[d(CGCG)r(UAUA)d(CGCG)]_2$, as well as their pure RNA and pure DNA duplex analogues. We have documented that, for identical sequences, the base (H8/H6) and H1′ protons of RNA duplexes have longer nonselective T_1s than those of DNA, by factors of 2–3-fold. The reason for choosing nonselective rather than selective inversion–recovery experiments was the realization that, in large molecules, the initial magnetization after a *selective* inversion pulse rapidly equilibrates throughout the spin system via the dominant zero-quantum cross-relaxation term (Solomon, 1955):

$$\frac{1}{T_1} = \sum_{S \neq I} \frac{\hbar^2 \gamma_I^2 \gamma_S^2}{20 r_{IS}^6} [J_0(\omega_I - \omega_S) + 3J_1(\omega_I) + 6J_2(\omega_I + \omega_S)] \quad (2)$$

At the same time, all the spins are also relaxing via leakage to the lattice, albeit at a slower rate that depends upon the amplitude and rate of local dynamics. In contrast, in a *non*selective inversion–recovery experiment, zero-quantum cross-relaxation is at a minimum immediately after the inversion pulse (eq 1) since, ideally, all the spins are polarized in the same direction and relaxation initially occurs primarily through leakage to the lattice via single- and double-quantum transitions (Kalk & Berendson, 1976). Hence the nonselective inversion–recovery experiment is, at least initially, more sensitive to high-frequency motions (i.e., internal motions) than the selective inversion–recovery experiment. Our H5–H6 cross-relaxation buildup rates (Figure 7) show no evidence of large differences in internal motion between DNA and RNA, indicating that the T_1 differences between DNA and RNA are due to structural rather than to motional differences. However, it is important to note that the NOE experiment is heavily dominated by J_0, and it might still be possible that differences in picosecond-to-nanosecond internal motions exist between DNA and RNA that are too small to change the dominant $J_0(\omega_I - \omega_S)$ component but significant enough to cause differences in $J_1(\omega_I)$ and $J_2(\omega_I + \omega_S)$. Thus small differences in internal motion might still exist and contribute to the observed nonselective T_1 (eq 1) differences without detectably changing the initial rate of the NOESY buildup. Nevertheless, since it is the time-dependent NOESY data set which provides the cross-relaxation rates from which distances are extracted, our results show that any internal motion differences between DNA and RNA can be safely ignored in structure determination of DNA–RNA chimeras and hybrids. The longitudinal relaxation differences between DNA and RNA cannot, on the other hand, be overlooked and must be taken into account when determining the relaxation delay in time-dependent NOESY experiments on DNA–RNA hybrids and chimeras.

Documenting the extent of the internal motion contribution will require further analysis of the data using various motional models and actual duplex structures rather than averaged fiber-diffraction coordinates. Furthermore, nonselective T_1s, even at moderately early time points, probably contain significant $J_0(\omega_I - \omega_S)$ contamination and may not be valid targets for fine tuning internal motion contributions. From the foregoing, it is obvious that extracting the dynamic properties of nucleic acid polymers from proton relaxation data in solution is a difficult and complicated process due to the contributions of both structure and dynamics to the relaxation processes. Site-specific deuterium relaxation [which is independent of proton spin density (Brandes et al., 1990)] is a much superior approach to monitoring dynamic differences, and such studies are in progress.

Because of the 2–3-fold slower RNA longitudinal recovery, studies on DNA–RNA hybrids or chimeras must use recycle delays sufficiently long such that the equilibrium magnetization of the RNA protons is within 10% of that of the DNA protons in order to avoid serious errors in distance estimates caused by differential partial saturation of, and consequently weaker NOE cross-peaks from, RNA protons. For the typical RNA–DNA T_1 values of ~5–~2 s observed in this study, achieving recovery values of ca. 91.8% for RNA and 99.8%

for DNA will require 12–13 s of relaxation delay during signal averaging. This will increase the time required to collect a single phase-sensitive 32-scan NOESY experiment (with 400 t_1 points) to ca. 3.5 days, or 2 weeks for a four-point NOE buildup. Thus, while the bad news is that RNA–DNA hybrid/chimera studies will require large amounts of spectrometer time to generate distance data, the good news is that the differences in internal motion (if any) between DNA and RNA are not large enough to cause observable differences in R_C and do not introduce significant distance errors into the structure calculations for RNA duplexes, DNA–RNA hybrids, and chimeric d–r–d duplexes. Conversely, NOESY spectra collected with the shorter 1–3-s relaxation delays frequently used for DNA studies (Nilsson et al., 1986, 1987; Nerdal et al., 1989; Baleja et al., 1990; Metzler et al., 1990; Gmeiner et al., 1990; Macaya et al., 1991; Kouchakdjian et al., 1991) will produce serious distance errors due to the partial saturation of RNA protons. This includes not only internal distances within the RNA segment but also DNA to RNA distances at the junction whose structure is being studied; such cross-peaks appear as inherently nonsymmetrical NOE intensities above and below the diagonal when one component is incompletely relaxed.

Acknowledgments

We thank Drs. J. Michael Schurr, Gary P. Drobny, Bryant Fujimoto, Jeff Davis, and Miguel Salazar for valuable discussions. We thank David Gregory for assistance with proton density calculations. We also thank Susan Ribeiro and Julie Miller for DNA/RNA synthesis and Mary Coventry for manuscript preparation. A.C.W. acknowledges a NIH predoctoral traineeship from Molecular Biophysics Training Grant GM08268-04.

References

Arnott, S., & Hukins, D. W. L. (1972a) *Biochem. Biophys. Res. Commun. 47*, 1504–1509.

Arnott, S., & Hukins, D. W. L. (1972b) *Biochem. Biophys. Res. Commun. 48*, 1392–1399.

Baleja, J. D., Pon, R. T., & Sykes, B. D. (1990) *Biochemistry 29*, 4828–4839.

Brandes, R., Vold, R. R., Kearns, D. R., & Rupprecht, A. (1990) *Biochemistry 29*, 1717–1721.

Cech, T. R., & Bass, B. L. (1986) *Annu. Rev. Biochem. 55*, 599–629.

Chou, S. H., Flynn, P., & Reid, B. R. (1989) *Biochemistry 28*, 2422–2435.

Chou, S. H., Flynn, P., Wang, A. C., & Reid, B. R. (1991) *Biochemistry 30*, 5248–5257.

Ernst, R. R., Bodenhausen, G., & Wokaun, A. (1987) in *Principles of Nuclear Magnetic Resonance in One and Two Dimensions* (Breslow, R., Ed.) Oxford University Press, New York.

Gmeiner, W. H., Rao, K. E., Rayner, B., Vasseur, J.-J., Morvan, F., Imbach, J.-L., & Lown, J. W. (1990) *Biochemistry 29*, 10329–10341.

Green, P. J., Pines, O., & Inouye, M. (1986) *Annu. Rev. Biochem. 55*, 569–597.

Guerrier-Takada, C., Gardiner, K., Marsh, T., Pace, N., & Altman, S. (1983) *Cell 35*, 849–857.

Hare, D. R., Wemmer, D. E., Chous, S. H., Drobny, G., & Reid, B. R. (1983) *J. Mol. Biol. 171*, 319–336.

Hoffman, M. (1991) *Science 254*, 379.

Huang, W.-C., Orban, J., Kintanar, A., Reid, B. R., & Drobny, G. P. (1990) *J. Am. Chem. Soc. 112*, 9059–9068.

Ivanov, V. I., Minchenkova, L. E., Schyolkina, A. K., & Poletayev, A. I. (1973) *Biopolymers 12*, 89–110.

Kalk, A., & Berendson, H. J. C. (1976) *J. Magn. Reson. 24*, 343–366.

Kintanar, A., Klevit, R. E., & Reid, B. R. (1987) *Nucleic Acids Res. 15*, 5845–5862.

Kouchakdjian, M., Eisenberg, M., Johnson, F., Grollman, A. P., & Patel, D. J. (1991) *Biochemistry 30*, 3262–3270.

Levitt, M. H., & Freeman, R. (1981) *J. Magn. Reson. 43*, 65–80.

Macaya, R. F., Gilbert, D. E., Malek, S., Sinsheimer, J. S., & Feigon J. (1991) *Science 254*, 270–274.

McMullan, R. K., & Craven, B. M. (1989) *Acta Crystallogr. B45*, 270–276.

Metzler, W. J., Wang, C., Kitchen, D. B., Levy, R. M., & Pardi, A. (1990) *J. Mol. Biol. 214*, 711–736.

Nerdal, W., Hare, D. R., & Reid, B. R. (1989) *Biochemistry 28*, 10008–10021.

Nilges, M., Clore, G. M., & Gronenborn, A. M. (1987) *Biochemistry 26*, 3718–3733.

Nilsson, L., Clore, G. M., Gronenborn, A. M., Brünger, A. T., & Karplus, M. (1986) *J. Mol. Biol. 188*, 455–475.

Ogilvie, K. K., Usman, N., Nicoghosian, K., & Cedergren, R. J. (1988) *Proc. Natl. Acad. Sci. U.S.A. 85*, 5764–5768.

Peticolas, W. L., Wang, Y., & Thomas, G. A. (1988) *Proc. Natl. Acad. Sci. U.S.A. 85*, 2579–2583.

Rhodes, D., & Klug, A. (1986) *Cell 46*, 123–132.

Solomon, I. (1955) *Phys. Rev. 99*, 559–565.

States, D. J., Haberkorn, R. A., & Ruben, D. J. (1982) *J Magn. Reson. 48*, 286–292.

Wang, A. C., Kim, S. G., Flynn, P. F., Sletten, E., & Reid, B. R. (1992) *J. Magn. Reson.* (in press).

Wang, Y., Thomas, G. A., & Peticolas, W. L. (1987) *J. Biomol. Struct. Dyn. 5*, 249–274.

Weber, H. P., Craven, B. M., & McMullan, R. K. (1980) *Acta Crystallogr. B36*, 645–649.

Wickner, R. B. (1986) *Annu. Rev. Biochem. 55*, 373–395.